MASTER

Conf-790709--3

PREPRINT UCRL- 82614

Lawrence Livermore Laboratory

ELASTIC AND PLASTIC PROPERTIES OF URANIUM DIOXIDE FROM 5 TO 330 GPa

W. H. Gust

May 14, 1979

This paper was prepared for submittal to the Proceedings of the Seventh AIRAPT International High Pressure Conference, Le Cruset, France, July 30 to August 3, 1979.

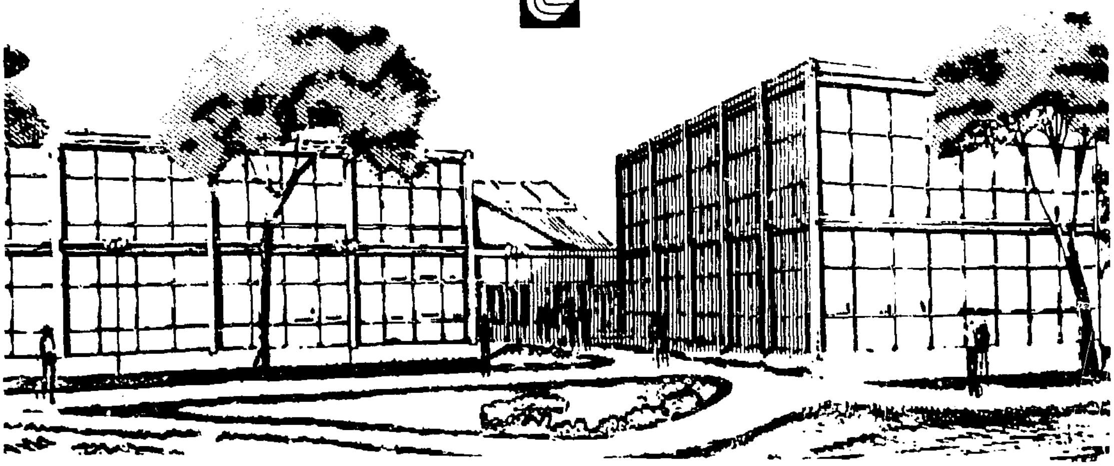

ELASTIC AND PLASTIC PROPERTIES OF URANIUM DIOXIDE FROM 5 TO 330 GPa*

W. H. Gust

University of California, Lawrence Livermore Laboratory

Livermore, CA 94550

ABSTRACT

Published Hugoniot data for UO_2 is in error, because the measuring techniques used did not resolve the strong multiple-wave shock-structures present. Hence calculations related to liquid metal, fast-breeder-reactor, excursion analyses based on extrapolations of that data are in serious error. We have used the inclined prism, flash gap, and two-stage gas-gun techniques to determine shock-compression parameters for UO_2 to 330 GPa. The Hugoniot elastic limit for UO_2 was found to be 5.7 GPa. At higher pressure, a plot of shock vs particle velocity displays a discontinuity between $1.0 < U_p < 1.8$ km/s, which appears to be a manifestation of a solid-solid phase transition. For $1.8 < U_p < 4.0$ km/s, the plot is given by $U_s = 5.8 + 1.28 (U_p - 1.8)$. In this regime, both the elastic and phase transitional waves have been overdriven so the curve may be validly extrapolated to higher values. This curve differs substantially from those previously reported.

*Work performed under the auspices of the U. S. Department of Energy by Lawrence Livermore Laboratory under contract No. W-7405-Eng-48.

INTRODUCTION

The study of the properties of solid and molten uranium dioxide (UO_2) is of considerable current interest in the field of liquid metal, fast-breeder-reactor, excursion analyses. A fundamental requirement is the determination of reliable shock-compressed pressure-volume data for full-density fuel material. These data are essential for the extrapolations that permit calculations of material behavior during the transition from a dense solid to a molten liquid. A reliable equation of state that includes these phenomena provides the necessary link between the coupled hydrodynamic and neutronics codes.

Conventional shock-velocity measurements on materials that exhibit strong elastic waves under shock compression, (i.e., UO_2) are often erroneous in the low-pressure region. This is because the flash gap and biased electrical pin shock-velocity measurement techniques usually employed do not resolve the multiple-wave shock structures involved. Consequently, extrapolations based on such data are not valid.

Several shock-wave measurement techniques are capable of resolving multiple-wave shock structures up to about 50 GPa. Among these are the capacitor, manganin gage, inclined mirror, and inclined prism techniques. We used inclined prisms [1,2] to about 50 GPa to resolve the two-wave shock structure related to the Hugoniot elastic limit (HEL) of UO_2. Experiments at plastic-wave velocities great enough to overdrive the elastic wave (50 to 150 GPa) were done with flash gap systems [3] (reverberations within the high velocity, explosively driven, flying plates used to obtain the high pressure made the use of inclined prisms inappropriate). Data from 150 to 330 GPa were obtained with a two-stage light-gas gun [4].

In this investigation, we have applied a shock-wave measurement technique capable of resolving multiple-wave shock structures related to a strong elastic wave. Further, we have attempted to clarify Hugoniot parameters in a previously unreported transition region as well as in a regime of considerably higher pressure.

PROCEDURE

Brittle materials often exhibit multiple-wave shock structures during the compressive pulse. The initial wave may be an elastic wave that propagates roughly at the longitudinal speed of sound and compresses the material up to the plastic yield point (Hugoniot elastic limit). If a pressure-induced polymorphic transition occurs, the second wave brings the pressure in the material up to the point of transformation. The transformation occurs in the third wave, which takes the material to the final state achieved in a given experiment. A number of experiments at different pressure levels serve to provide a locus of shock-velocity and particle-velocity points from which pressure-volume and energy-volume states may be derived.

Use of inclined prisms to resolve multiple waves is not appropriate in experiments where compression is obtained through use of explosively driven flying plates (e.g., systems G-I, Table I). This is because reverberations within the explosively driven flyer may launch additional extraneous waves into the sample and may cause error. Hence in this pressure regime, the flash-gap technique [3], which is relatively insensitive to the flyer plate reverberations, was used. If the material transforms in this regime, the usual procedure is to identify the transition point through discontinuities in plots of shock-compression variables, e.g., shock velocity vs particle velocity.

In the experiments done on the gun, 1.5 mm-thick plates of Ta were impacted on 25.4-mm-diam by 3.2-mm-thick UO_2 samples. The geometry used is shown schematically in Fig. 1. Six foil switches were bonded radially (~1 μ of epoxy) onto the sample at 60-deg intervals; they were made of

12-μm-thick manganin foils enclosed in 12-μm-thick Mylar.* Total thickness of a foil switch was about 30 μm. An 0.8-mm-thick Ta shim was bonded to the front side of the foil switch array to protect them from possible pre-impact damage by hot gases.

On the back side of each sample, six coaxial self-shorting pins were placed in contact with the UO_2 sample on a 12.7-mm-diam array so that each was directly in line with a foil switch, thereby reducing the effect of impactor tilt. A seventh pin was located at the center. The foil switches were biased to 150 V. Conventional corrections were made to account for shock transit time through the end walls of the brass pin and the gaps between the end walls and the inner conductors.

Upon impact, the resulting pulses were recorded on 10 oscilloscopes arranged in 5 master-slave systems. Oscilloscope non-linearity was accounted for by placing an accurately known sine wave (10 ns/cycle) on each oscilloscope record. Small corrections were made to account for differences in signal-transmission line length and pin-closure times by conventional methods. No corrections for impactor tilt were made.

Compression parameters were determined through impedance matches that were centered on the Hugoniot for Ta [6] , with Ta particle velocity equal to one-half the projectile velocity. Total uncertainty in the measurements is estimated to be less than 1.5%.

---

*Reference to a company or product name does not imply approval or recommendation of the product by the University of California or the U. S. Department of Energy to the exclusion of others that may be suitable.

For multiple waves, stress and volume are given by

$$\sigma_n = V_{n-1}^{-1}(U_{s_n} - U_{p_{n-1}}) \quad (U_{p_n} - U_{p_{n-1}}) + \sigma_{n-1}$$

and

$$V_n = V_{n-1} \, (U_s - U_{p_n})/(U_{s_n} - U_{p_{n-1}}).$$

The particle velocity for the elastic wave was obtained from the free-surface approximation, i.e., $2\,U_{p_1} = U_{fs_1}$. For the experiments done with inclined prisms, U_{p_2} was determined from the free-surface approximation and from impedance matching. The method used to obtain a graphical solution to an impedance match when multiple waves are present is shown in Fig. 2.

MATERIALS

The high-purity samples of uranium dioxide ($UO_{2.02}$ actually) used in these experiments were manufactured by the Nuclear Division of Union Carbide Corporation.

The uranium was obtained as a precipitate from a uranyl nitrate solution. The precipitate gel was calcined to UO_3, after which the UO_3 was reduced to UO_2 with hydrogen at about 675 K. The UO_2 powder was then isostatically cold pressed at 100 MPa, followed by sintering at 2075 K for 2 h.

This process produced samples that were from 95 to 97% of theoretical density (10.86 Mg/m^3). Spectrographic and chemical analyses on typical samples indicated about 80 other elements were present in very small amounts, i.e., a few parts per million or less. Total impurities present were less than 0.015 at.%.

The inclined-prism experiments were performed with slabs that were 50.8 mm x 25.4 mm x 6.4 mm in size. The samples for the flash-gap experiments were disks 19.0 mm in diameter and 6.4 mm thick. Samples used in the experiments were 19.0 mm in diameter and 3.2 mm thick. The major surfaces of all samples were flat and parallel within 5 μm.

RESULTS

The results are summarized in Table II and displayed in Fig. 2. The Hugoniot elastic limit was found to be about 5.7 GPa. Linear relations between shock and particle velocities were found for two regimes. The low-pressure data can be described by $U_s = 3.88 + 1.11\ (U_p - 0.3)$ for $0.3 < U_p < 1.05$ km/s. At higher pressure, the plot displays a discontinuity for $1.05\ U_p < 1.8$ km/s. The final segments are described by $U_s = 5.30 + 1.28\ (U_p - 1.8)$ for $1.8 < U_p < 4.0$ km/s.

DISCUSSION

The results in Table II and in Figs. 3 and 4 indicate that UO_2 exhibits a strong, relatively fast, elastic wave under shock compression. The amplitude of the Hugoniot elastic limit (5.7 GPa) was obtained from four excellent photographic records; all four displayed changes in slope that are characteristic of two-wave shock structures (see Fig. 4, a typical example). The velocity of the elastic wave was in good agreement with our ultrasonically measured, longitudinal sound speed at 1 atm (5.26 vs 5.19 km/s). This measurement was made on samples used in the inclined-prism experiments. Note in Table II that samples used for the high-pressure gun experiments were about 1% less dense but had drastically different elastic properties ($C_L \cong 4.71$ km/s).

In the U_s, U_p plot (Fig. 3), the line segment that represents the low-pressure regime does not extrapolate to bulk sound speed at $U_p = 0$ km/s, which is an indication of irregular behavior at low pressure. Good agreement between C_L and U_{s_1} indicates that third-order elastic effects are probably not responsible. For normal materials in the low-pressure regime, the particle velocity obtained from an impedance match with the plastic wave is very nearly equal to or slightly less (1%) than half the free-surface velocity, i.e., $U_{p_2} = U_{fs_2}/2$. However, the data in Table II for systems A to D indicate that U_{fs_2} is 14 to 20% less than two U_{p_2}, thus providing additional evidence of anomalous behavior in that regime.

At higher pressure, the plot displays a discontinuity for $1.1 < U_p < 1.8$ km/s ($\sigma \simeq 52.5$ GPa). This is probably a manifestation of a phase transition. Such discontinuities are usually considered to be related to unusual material behavior, i.e., phase transitions, and represent a mixed-phase region. Uranium dioxide has the cubic fluorite crystallographic structure. It may be recalled that several substances with this structure transform to the orthorhombic $PbCl_2$ structure under static high pressure [7]. For example, this transition occurs between 2.7 and 11.0 GPa for BaF_2, CaF_2, SrF_2 and EuF_2 [8, 9].

For $2.1 < U_p < 2.3$ km/s, our data agree fairly well with those of Goplen [10]. In this regime, the elastic wave is overdriven so that flash gap results are valid. The discontinuities at 1.9 to 2.0 km/s probably mark the points where the phase transitional waves have been overdriven.

The final part is described by $U_s = 5.28 + 1.28\,(U_p - 1.8)$ km/s for $1.8 < U_p < 4.0$ km/s. This portion does not extrapolate back to C_B, the bulk sound speed at $U_p = 0$, which provides additional evidence that at least one phase transition has occured. In this regime, both the elastic and phase transitional waves have been overdriven so that the curve may be validly extrapolated to higher values.

Our low-pressure results shown in Fig. 3, do not agree well with those of Goplen [10] and of Allen _et al._ [11]. The reason apparently is that their results are erroneous, because they did not use measuring techniques capable of resolving strong multiple-wave shock structures.

Goplen's measurements were done with the flash gap technique. These measurements are based upon intense light pulses resulting from shock reverberations that occur when shocked free surfaces of the baseplate and sample close small gas-filled gaps. When a strong elastic wave reaches the free surface first, the free surface advances slowly (but no flash occurs) while at the same time a simple backwards-facing rarefaction wave proceeds into the compressed material where it may interact with and degrade the advancing main shock. Hence the signal produced when the plastic wave finally flashes the gap is in error because of the boundary change caused by the advance of the free surface and by the degradation of the plastic wave by the rarefaction wave. Under these circumstances, namely, in the presence of a strong elastic wave, the flash gap measurements usually indicate values that are too low until the shock is of sufficient strength to overdrive the elastic wave.

Goplen's low-pressure results ($0.6 < U_p < 2.0$ km/s) apparently fall into this category. His results for $2.2 < U_p$ km/s, where the elastic wave is overdriven, agree with ours. His data, however, suffer from the fact that he was unable to obtain pressures high enough to completely overdrive the phase transitional wave, and his final results were obtained in a mixed phase regime. Hence his extrapolation based on his highest pressure data and on sound speed at zero pressure ($U_s = 4.4 + 0.8\ U_p$) for crystal-density material is not valid (sound speed for the transformed material is not known).

The capacitance-technique experiments performed by Allan et al. [11] were not done at high enough pressure (4.2 GPa) to exceed the Hugoniot elastic limit and, therefore, did not display two wave-shock structures. Similar experiments with a final pressure twice as great should show it.

The electrical-shorting-pin technique used in their high explosively driven experiments was not capable of resolving two wave-shock structures.

Their recorded data indicate that the shock velocity measured in each case was probably for the elastic wave. In no case does the recorded shock velocity exceed their ultrasonically measured longitudinal sound speed (5.147 km/s). The elastic wave was evidently strong enough to trigger the shorting pins. Needless to say, the particle velocity obtained from a single wave impedance match with the brass standard and the elastic wave is incorrect, because it does not account for the plastic wave.

ACKNOWLEDGMENTS

The author thanks D. R. Mizer, J. G. Moore, and G. V. Seely for experiment construction; R. W. Brown, A. Donnici, L. F. Simmons, and E. Urquidez for aid at the high explosive test site; and D. J. Steinberg for support and helpful discussions.

NOTATION

C_B	=	bulk sound velocity
C_L	=	longitudinal sound velocity
C_S	=	shear sound velocity
n	=	order of successive waves
U_p	=	particle velocity
U_{fs}	=	material free-surface velocity
U_s	=	shock velocity
V	=	$1/\rho$ = volume
ρ	=	density
σ	=	stress

REFERENCES

1. G. Eden and P. W. Wright, in Proc. of Fourth Symposium on Detonation (Office of Naval Research, Washington, D. C., 1965), p. 573.
2. W. H. Gust and E. B. Royce, J. Appl. Phys. 42, 276 (1971).
3. R. N. Keeler and E. B. Royce, in Physics of High Density, P. Caldirola and H. Knopfel, Eds. (Academic Press, New York, 1971) p. 51.
4. For a more detailed description see, D. R. Christman, W. M. Isbell, S. G. Babcock, A. R. McMillan, and S. J. Green, General Motors, Lab. Report MSL-70-23, Vol. II (or DASA 2501-2) (1971).
5. B. M. Dobratz, Lawrence Livermore Laboratory, Report UCRL-5139 Rev. 1 (1974).
6. J. J. Folkins and W. H. Gust, Bull. Am. Phys. Soc. 20, 1514 (1975).
7. W. F. T. Pistorius, Prog. Solid State Chem. 11, 72 (1976).
8. K. Siefort, Fortschr, Miner. 45, 214 (1968).
9. G. A. Samara, Phys. Rev. B, 2, 4194 (1970).
10. B. Goplen, Los Alamos Scientific Laboratory, Report LA-4319 (1969).
11. J. W. S. Allan, N. E. Hoskin, E. Morris, and P. H. White, Thermodynamics of Nuclear Materials, Vol. 1 (International Atomic Energy Agency, Vienna, 1975), p. 253.

Table I. Shock generating systems. All systems consisted of a 0.3-m-diam plane-wave lens with a 0.3-m right cylinder of high explosive, 0.15 m long. All attenuator components were flat and parallel within 5 μm.

System	Shock generator[a]	Attenuator and base-plate materials	Component thickness (mm)	Pressure in baseplate (± 5%, GPa)
A	Pressed TNT	Brass	25.4	11.7
		Lucite	12.7	
		OFHC Copper	12.7	
B	Pressed TNT	OFHC Copper	12.7	30.0
C	PBX 9205 (RDX)	Brass	12.7	43.0
D	PBX 9404 (HMX)	Brass	12.7	49.5
E	Pressed TNT	Air	3.0	94.6
		Monel	3.0	
		Air	25.4	
		Brass	4.8	
F	PBX 9205 (RDX)	Same as E	Same as E	135
G	PBX 9404 (HMX)	Same as E	Same as E	144
H	Two-stage gun	Ta flyer	1.5	200-400

[a]For a complete chemical description of these pressed and plastic-bonded explosives, see Ref. 5.

Table II. Data summary for uranium dioxide, UO_2.

Shock generating system	Baseplate: Free-surface or shock velocity (km/s)	Baseplate: Stress in standard (GPa)	Initial density (Mg/m^3)	Sound speed at 1 atm: C_L (km/s)	Sound speed at 1 atm: C_s (km/s)	Elastic regime: Shock velocity U_{s1} (km/s)	Elastic regime: Free-surface velocity U_{fs1} (km/s)	Elastic regime: Stress σ_1 (GPa)	Elastic regime: Volume V_1 (m^3/Mg)	Deformational regime: Shock velocity U_{s2} (km/s)	Deformational regime: Free-surface velocity U_{fs2} (km/s)	Deformational regime: Particle velocity U_{p2} (km/s)	Deformational regime: Final stress σ_2 (GPa)	Deformational regime: Volume V_2 (m^3/Mg)
A	0.3[a]	11.7	10.51	5.04	2.65	5.32	0.22	6.1	0.093	3.85	0.48	0.28[b]	12.7	0.0890
B	1.37[a]	30.0	10.54	5.19	2.69	5.27	0.16	4.3	0.093	4.47	1.14	0.66[b]	31.6	0.0852
C	1.97[a]	43.0	10.52	5.19	2.69	5.21	0.22	6.0	0.093	4.58	1.46	0.93[b]	45.3	0.0760
D	2.24[a]	50.5	10.54	5.20	2.69	5.25	0.24	6.6	0.093	4.79	1.75	1.05[b]	53.6	0.0743
D	5.33[c]	49.1	10.55	-	-	-	not measured		-	4.83	-	1.03	52.2	0.0826
E	6.29[c]	94.6	10.57	-	-	-	overdriven		-	5.28	-	1.75	95.0	0.0632
F	6.97[c]	133	10.57	-	-	-	overdriven		-	5.75	-	2.22	135	0.0580
G	7.15[c]	144	10.57	-	-	-	overdriven		-	6.03	-	2.32	148	0.0582
H	5.08[d]		10.37	4.64	2.52	-	overdriven		-	6.74	-	2.98	209	0.0538
H	5.01[d]		10.36	4.74	2.56	-	overdriven		-	6.81	-	2.92	206	0.0552
H	5.64[d]		10.36	4.64	2.55	-	overdriven		-	7.24	-	3.28	246	0.0528
H	5.65[d]		10.31	4.74	2.57	-	overdriven		-	7.30	-	3.27	246	0.0535
H	6.16[d]		10.36	4.69	2.56	-	overdriven		-	7.66	-	3.56	283	0.0516
H	6.24[d]		10.29	4.77	2.60	-	overdriven		-	7.72	-	3.62	287	0.0516
H	6.80[d]		10.35	4.70	2.55	-	overdriven		-	8.14	-	3.89	329	0.0504
H	6.84		10.37	4.64	2.52	-	overdriven		-	8.01	-	3.95	328	0.0489

[a] Inclined prism data; impedance match based on the free-surface velocity measurement of Cu.

[b] U_p from impedance match.

[c] Flash gap data; impedance match based on shock velocity measurement of brass.

[d] Ta projectile velocity; impedance match based on $2\,U_{p_{Ta}} = U_{proj}$.

Figures

Fig. 1. Schematic of projectile and target. The Ta shim, UO_2 sample and outer conductors were at ground potential. The manganin foils and pin center conductors were biased to 150 V.

Fig. 2. Impedance-match solution in the pressure-particle velocity plane for a two-wave shock. Point A is determined from a measurement of the free-surface velocity of the Cu baseplate (its equation of state is well known). From the continuity of stress and particle velocity across the shock front it is known that the final (σ, U_p) state, point B, must lie somewhere along the shock reflection from point A. Point B must be determined from a two-step solution as shown. Point C portrays the amplitude of the Hugoniot elastic limit.

Fig. 3. Plot of shock velocity as a function of particle velocity for UO_2 ($\rho_0 = 10.5$ Mg/m^3). The discontinuities at $U_p = 0.9$ and 1.9 km/s are probably related to the initiation and completion of a pressure-induced phase transition. Note that the line segments do not extrapolate to C_B at $U_p = 0$.

Fig. 4. Inclined-prism record for uranium dioxide with shock-generating System A. Shock-front breakout from the baseplate is at t_0; t_1 is the arrival time of the elastic wave at the sample surface; t_2 is the arrival time of the main shock at the sample surface. Free-surface velocities are related to the slopes of the wide traces.

DYB/bg

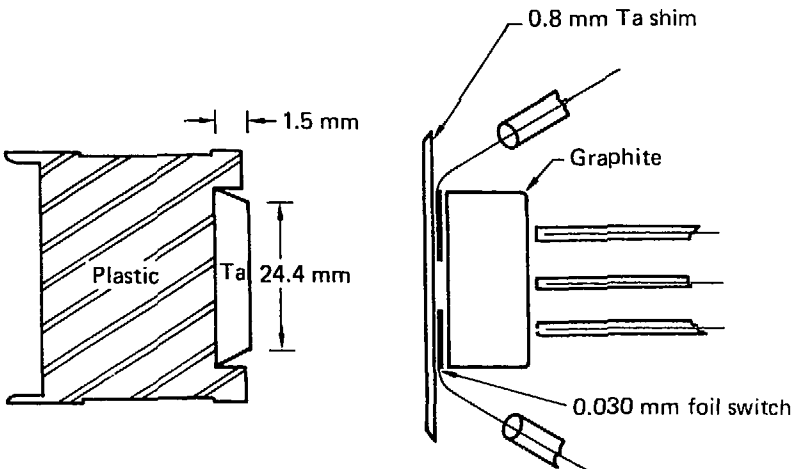

0.8 mm Ta shim
1.5 mm
Graphite
Plastic
Ta
24.4 mm
0.030 mm foil switch

Gust - Fig. 1

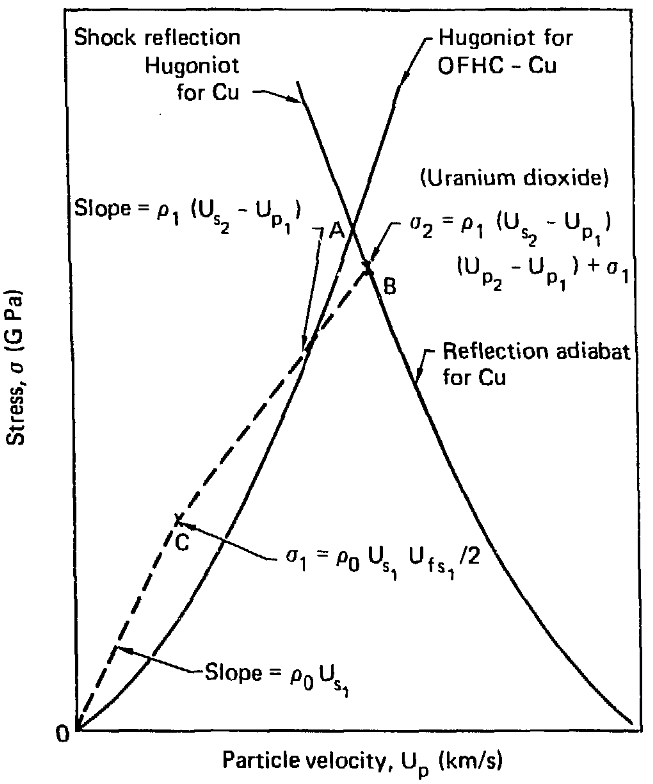

Shock reflection
Hugoniot
for Cu
Hugoniot for
OFHC - Cu
(Uranium dioxide)
Slope = $\rho_1 (U_{s_2} - U_{p_1})$
A
$\sigma_2 = \rho_1 (U_{s_2} - U_{p_1})$
$(U_{p_2} - U_{p_1}) + \sigma_1$
B
Reflection adiabat
for Cu
Stress, σ (G Pa)
C
$\sigma_1 = \rho_0 U_{s_1} U_{fs_1}/2$
Slope = $\rho_0 U_{s_1}$
0
Particle velocity, U_p (km/s)

Gust - Fig. 2

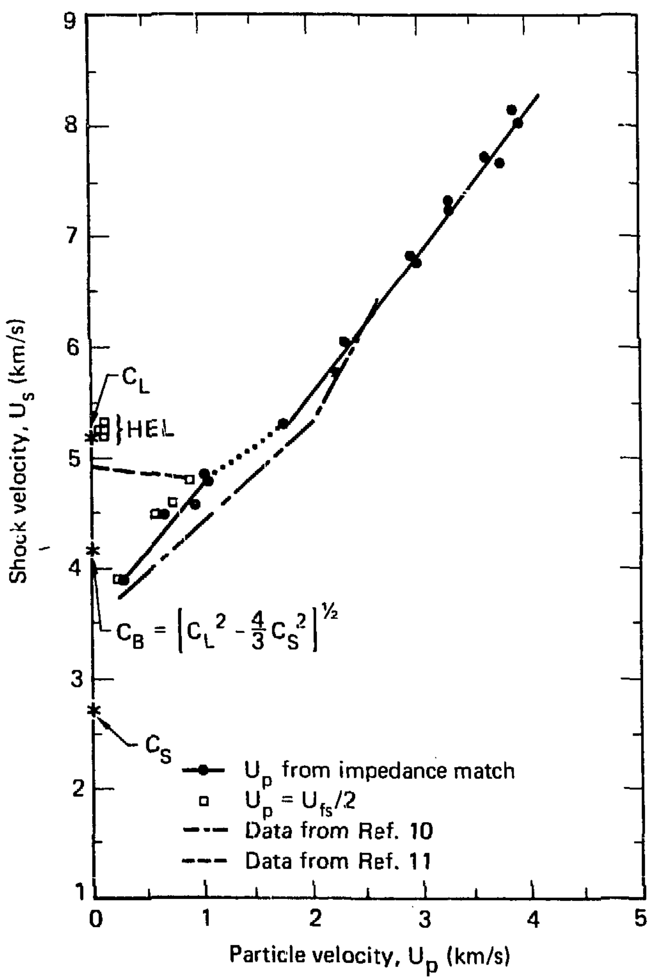

Shock velocity, U_s (km/s)
Particle velocity, U_p (km/s)
C_L
HEL
$C_B = \left[C_L^2 - \frac{4}{3}C_S^2\right]^{1/2}$
C_S
U_p from impedance match
$U_p = U_{fs}/2$
Data from Ref. 10
Data from Ref. 11

Gust - Fig. 3

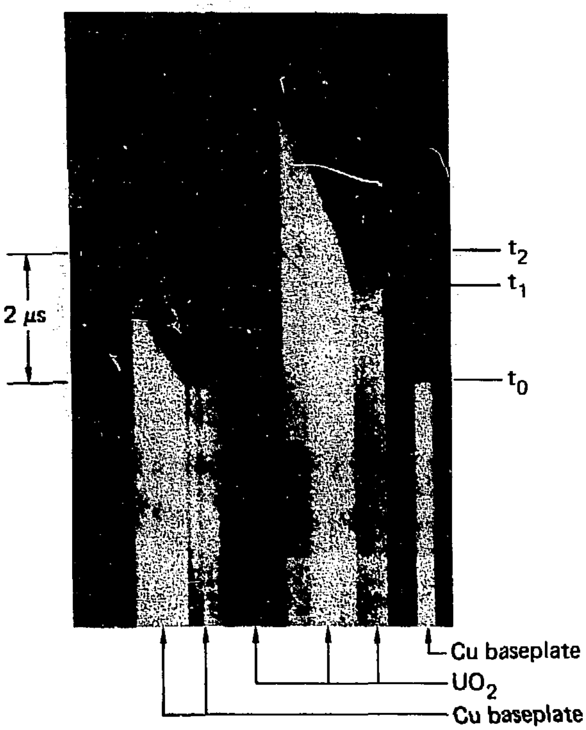

Gust - Fig. 4